Mode identification in rapidly rotating stars

D. R. Reese[1], M.-A. Dupret[2], and M. Rieutord[3]

[1]LESIA, [2]ULg, [3]IRAP
SISROT PNPS + ANR ESRR

27 March, 2018

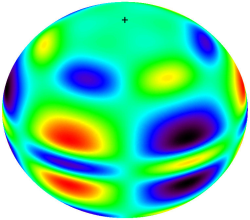

Introduction

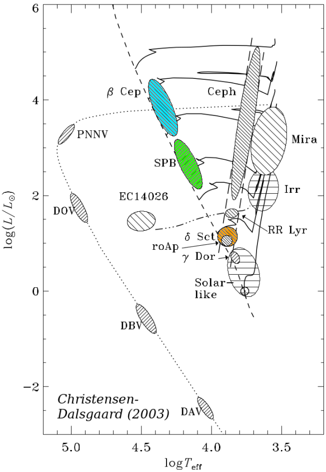

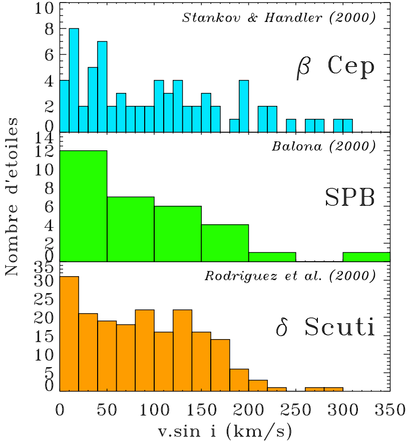

- many rapidly rotating pulsating stars

Introduction

Mode identification is difficult

- lack of *simple* frequency patterns, both in the observations and the theoretical expectations
- classical pulsators: no predictions for mode amplitudes

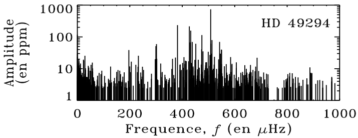

(Lefevre et al. 2009)

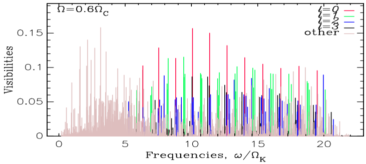

(Reese et al. 2013)

Introduction

Mode identification techniques

- photometric
  - amplitude ratios
  - phase differences
  - advantage: intrinsic amplitude factors out
- spectroscopic
  - Line Profile Variations (LPVs)
  - advantage: rich information content

Introduction

Mode identification techniques

- photometric
  - amplitude ratios
  - phase differences
  - advantage: intrinsic amplitude factors out
- spectroscopic
  - Line Profile Variations (LPVs)
  - advantage: rich information content

- the challenge: apply these techniques to rapid rotators

1. Introduction
2. Pulsations of rapidly rotating stars
   - Pulsation calculations
3. Ratios & phases
   - Calculating mode visibilities
   - Towards mode identification?
   - Amplitude ratios and phase differences
4. α Ophiuchi
5. Conclusion

Calculating mode visibilities and LPVs

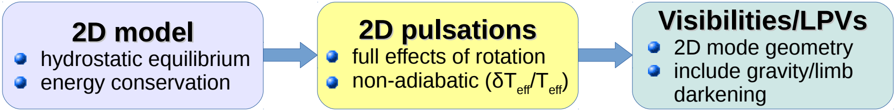

- non-adiabatic calculations needed for accurate $\delta T_{\text{eff}}/T_{\text{eff}}$ and phase differences
- energy conservation needed in model for non-adiabatic calculations

Rapidly rotating models

SCF models	ESTER models
Ω cylindrical	$\Omega(r,\theta)$
Barotropic	Baroclinic
Adiabatic	Non-adiabatic

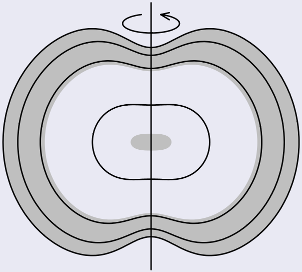

MacGregor et al. 2007

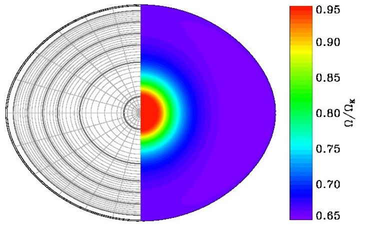

(Rieutord et al . 2016)

The TOP pulsation code

- TOP = Two-dimensional Oscillation Program
- fully includes centrifugal deformation
- can handle baroclinic models
- includes non-adiabatic effects

http://johnmannophoto.com/blog/?p=103

Island modes

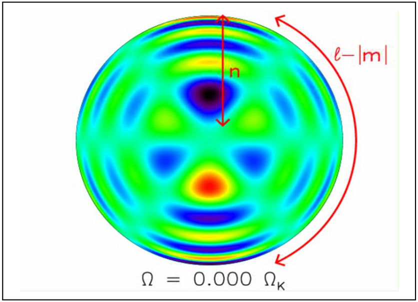

- new quantum numbers:

$$
\begin{aligned}
\tilde{n} &= 2n + \varepsilon, \\
\tilde{\ell} &= \frac{\ell - |m| - \varepsilon}{2}, \\
\varepsilon &\equiv \ell + m \; [2]
\end{aligned}
$$

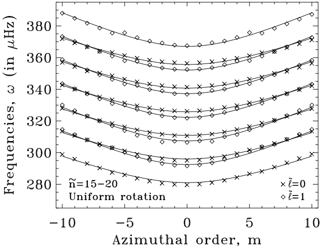

Reese et al., 2009

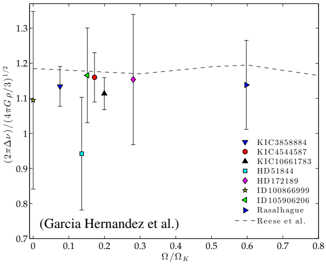

García Hernández et al. 2015

$$\omega_{\tilde{n},\,\tilde{\ell},\,\tilde{m}} \simeq \tilde{n}\Delta_{\tilde{n}} + \tilde{\ell}\Delta_{\tilde{\ell}} + m^2\Delta_{\tilde{m}} - m\Omega + \tilde{\alpha}$$

- $\Delta_{\tilde{n}}$ and $\Delta_{\tilde{\ell}} = \omega_{\tilde{\ell}+1} - \omega_{\tilde{\ell}}$ from ray dynamics (Lignières & Georgeot, 2008, 2009, Pasek et al. 2011, 2012)
- $\Delta_{\tilde{n}}$ scales with mean density (Reese et al. 2008, García Hernández et al. 2013)

1. Introduction
2. Pulsations of rapidly rotating stars
   - Pulsation calculations
3. Ratios & phases
   - Calculating mode visibilities
   - Towards mode identification?
   - Amplitude ratios and phase differences
4. α Ophiuchi
5. Conclusion

Calculating mode visibilities

Previous works

- Daszyńska-Daszkiewicz et al. (2002, 2007), Townsend (2003)
  - non-adiabatic treatment
  - approximate treatment of rotation
- Reese et al. (2013) (see also Lignières et al. 2006, Lignières & Georgeot 2009)
  - full treatment of rotation
  - adiabatic calculations
- Savonije (2013)
  - full treatment of Coriolis force, but no centrifugal deformation
  - non-adiabatic treatment
  - simplified visibilities

Equations

- non-pulsating star:

$$\mathcal{I} = \iint_{\mathrm{Vis.Surf.}} I(g_{\mathrm{eff}}, T_{\mathrm{eff}}, \mu)\vec{e}_{\mathrm{obs.}} \cdot d\vec{S}$$

- pulsating star:

$$\begin{aligned} \delta\mathcal{I} &= \xcancel{\iint_{\delta\mathrm{Vis.Surf.}} I(g_{\mathrm{eff}}, T_{\mathrm{eff}}, \mu)\vec{e}_{\mathrm{obs.}} \cdot d\vec{S}} \\ &+ \iint_{\mathrm{Vis.Surf.}} \delta I(g_{\mathrm{eff}}, T_{\mathrm{eff}}, \mu)\vec{e}_{\mathrm{obs.}} \cdot d\vec{S} \\ &+ \iint_{\mathrm{Vis.Surf.}} I(g_{\mathrm{eff}}, T_{\mathrm{eff}}, \mu)\vec{e}_{\mathrm{obs.}} \cdot \delta(d\vec{S}) \end{aligned}$$

Calculating visibilities

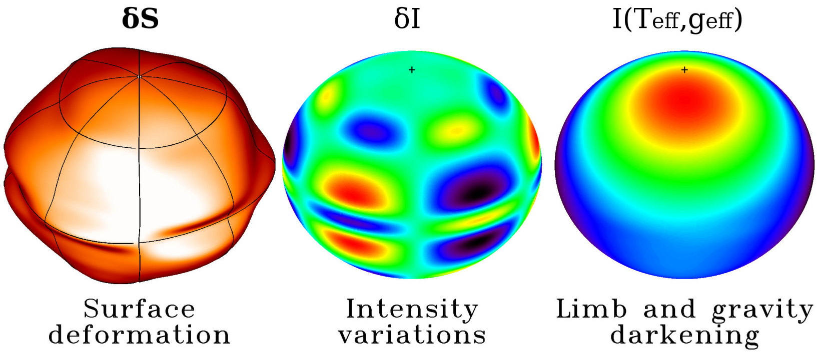

Intensities

BRITE red

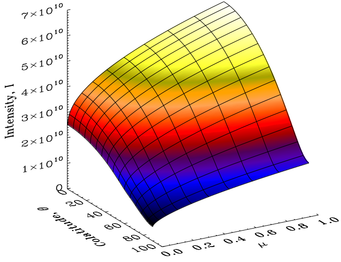

BRITE blue

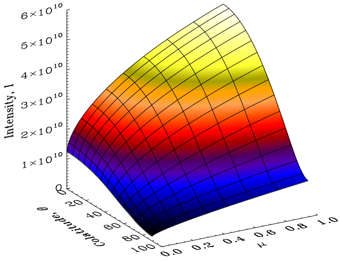

- intensities also available for other photometric systems

Amplitude ratios for the $n = 6$, $\ell = 2$ modes ($i = 30^\circ$)

$\Omega = 0.0\ \Omega_C$

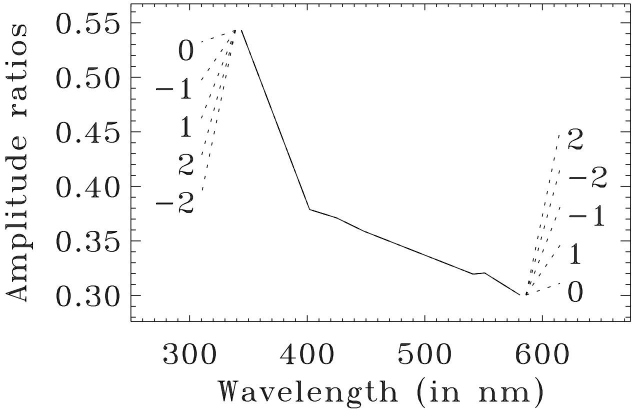

Amplitude ratios for the $n = 6$, $\ell = 2$ modes ($i = 30^\circ$)

$\Omega = 0.4\ \Omega_C$

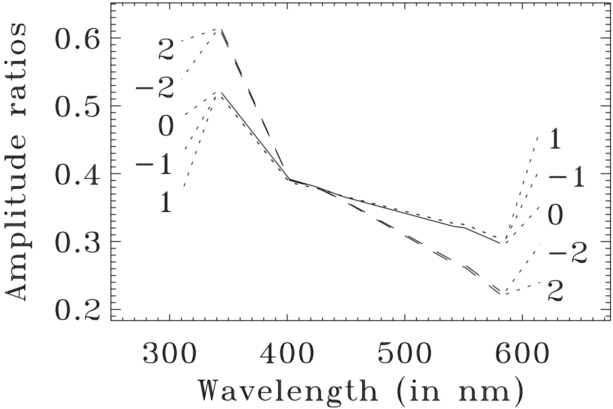

Amplitude ratios for the $n = 6$, $\ell = 2$ modes ($i = 30°$)

$\Omega = 0.8\ \Omega_C$

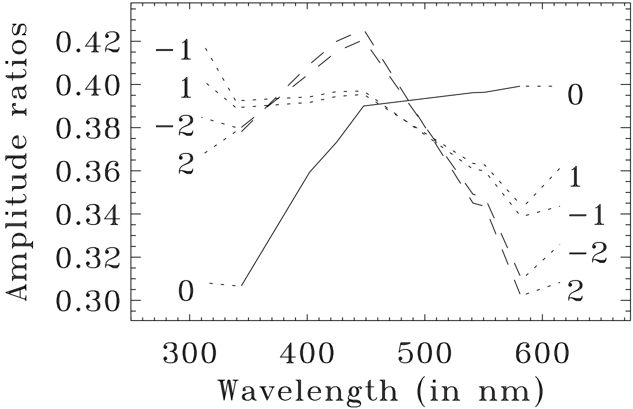

Amplitude ratios for the $\ell = 1$, $m = 0$ modes ($i = 60°$)

$\Omega = 0.0\ \Omega_C$

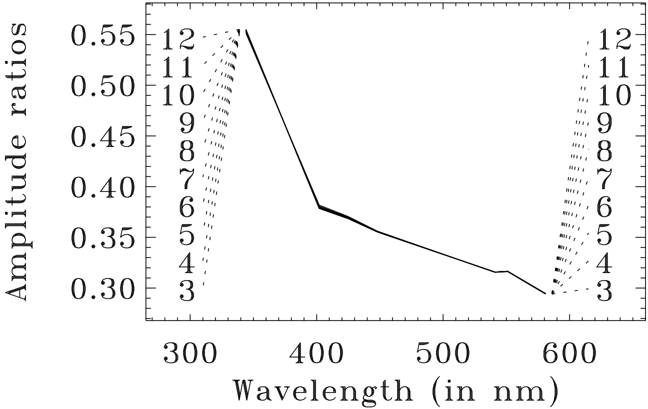

Amplitude ratios for the $\ell = 1$, $m = 0$ modes ($i = 60^\circ$)

$\Omega = 0.2\ \Omega_C$

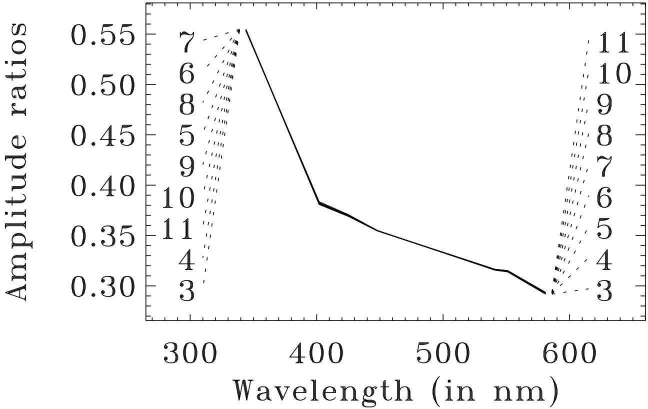

Amplitude ratios for the $\ell = 1$, $m = 0$ modes ($i = 60^\circ$)

$\Omega = 0.4\ \Omega_C$

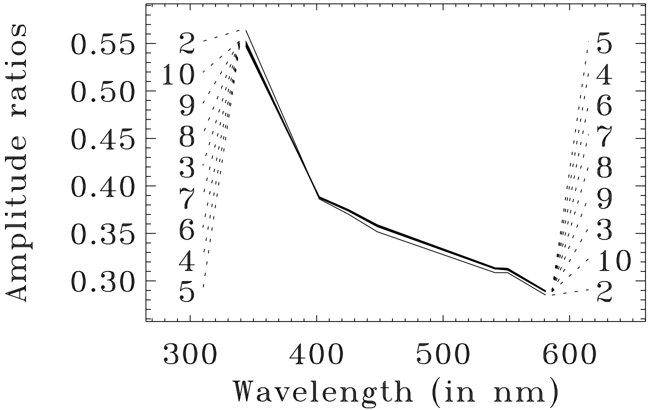

Amplitude ratios for the $\ell = 1$, $m = 0$ modes ($i = 60°$)

$\Omega = 0.6\ \Omega_C$

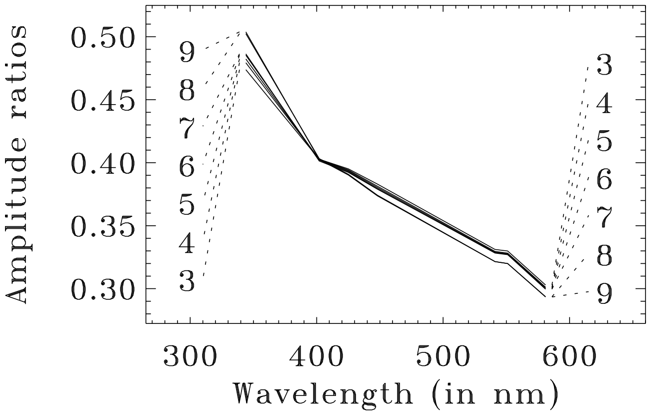

Amplitude ratios for the $\ell = 1$, $m = 0$ modes ($i = 60°$)

$\Omega = 0.8\ \Omega_C$

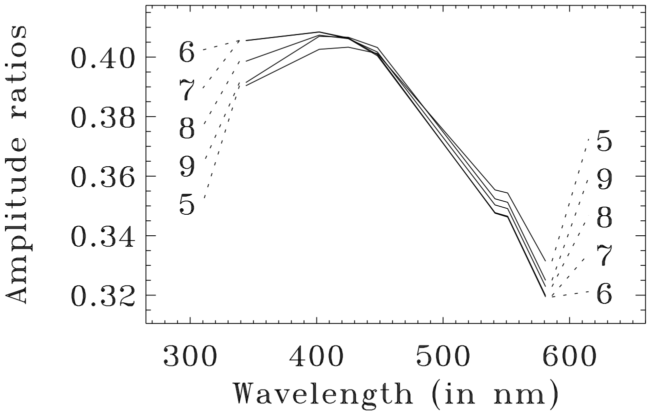

Towards mode identification?

- group modes together according to similar amplitude ratios
- hopefully you will get modes with similar quantum numbers
- similar structure expected from asymptotic ray theory (Pasek et al. 2012)

Multi-colour mode identification

Island mode, $(i=0°)$

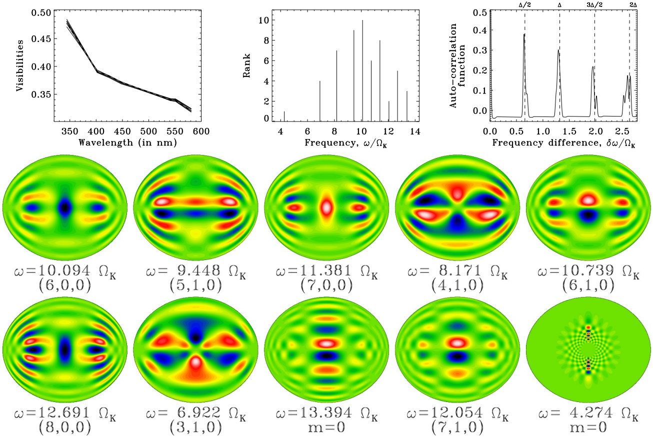

(see Reese et al. 2017)

- compare observed amplitude ratios between each other
  $\Rightarrow$ group modes with similar $(\ell, |m|)$ values

Multi-colour mode identification

Island mode, $(i = 60°)$

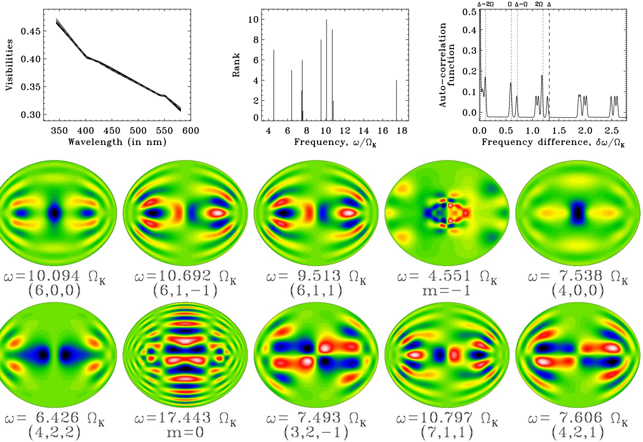

(see Reese et al. 2017)

- compare observed amplitude ratios between each other
  - $\Rightarrow$ group modes with similar $(\ell, |m|)$ values

Multi-colour mode identification

Model	Success	Isl. prop.
Ad. (2 $M_\odot$)	0.564	0.0115
Ad. (2 $M_\odot$)	0.145	0.0115
PNA (1.8 $M_\odot$)	0.469	0.0330
PNA (1.8 $M_\odot$)	0.201	0.0330

- PNA = pseudo non-adiabatic
- Geneva photometric system
- BRITE photometric system

Multi-colour mode identification

Model	Success	Isl. prop.
Ad. (2 $M_\odot$)	0.564	0.0115
Ad. (2 $M_\odot$)	0.145	0.0115
PNA (1.8 $M_\odot$)	0.469	0.0330
PNA (1.8 $M_\odot$)	0.201	0.0330

- PNA = pseudo non-adiabatic
- Geneva photometric system
- BRITE photometric system

Model	Success
BRITE	0.201
B, G	0.182
U, B, G	0.327
U, B1, B, G	0.380
U, B1, B, b2, G	0.437
U, B1, B, b2, V1, G	0.456
U, B1, B, b2, V1, V, G	0.469

Multi-colour mode identification

Summary

- above strategy works for
  - 3 or more colour bands
  - stars with many acoustic frequencies in asymptotic regime
  - hence, ideal for δ Scuti stars

Multi-colour mode identification

Summary

- above strategy works for
  - 3 or more colour bands
  - stars with many acoustic frequencies in asymptotic regime
  - hence, ideal for δ Scuti stars

- what about stars with few modes/few colours?

Amplitude ratios and phase differences

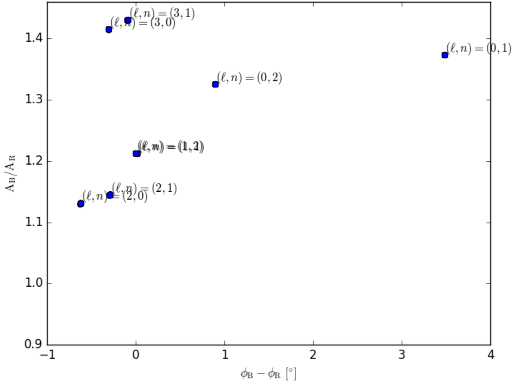

- Here: 9 $M_\odot$, $T_{\text{eff}} = 23493$, $\log g = 4.24$

Amplitude ratios and phase differences

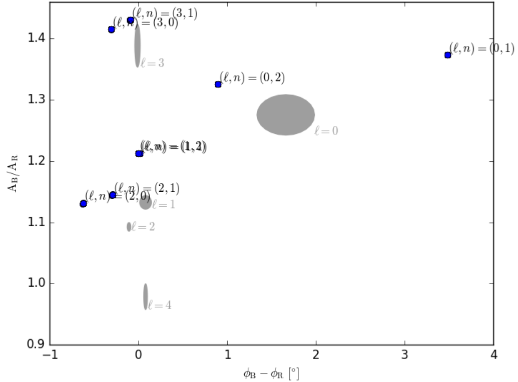

- Here: 9 $M_\odot$, $T_{\rm eff} = 23493$, $\log g = 4.24$
- Handler et al. (2017): 9.5-10 $M_\odot$, $T_{\rm eff} = 22000 \pm 600$ K, $\log g = 3.85 \pm 0.05$

Amplitude ratios and phase differences

$$\Omega = 0.1\Omega_{\mathrm{K}}$$

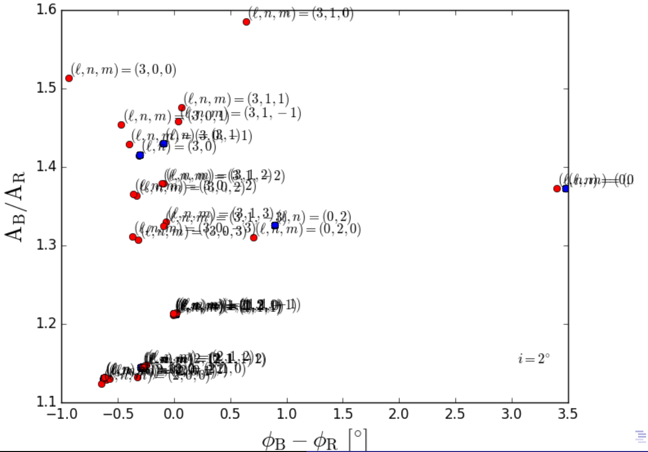

Amplitude ratios and phase differences

$$\Omega = 0.5\Omega_{\mathrm{K}}$$

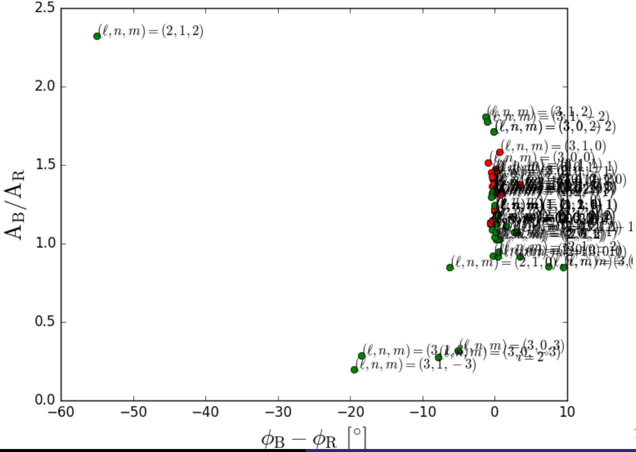

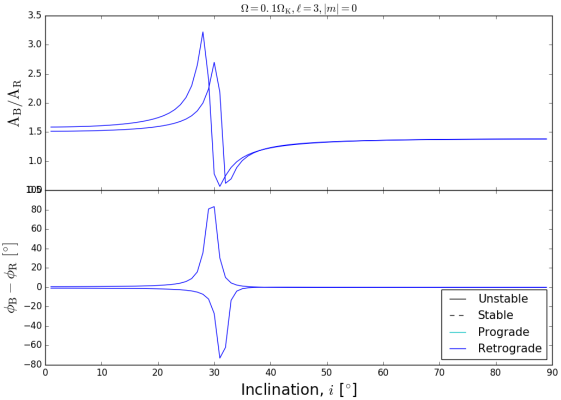

- sharp spikes result from amplitudes going to zero at different inclinations

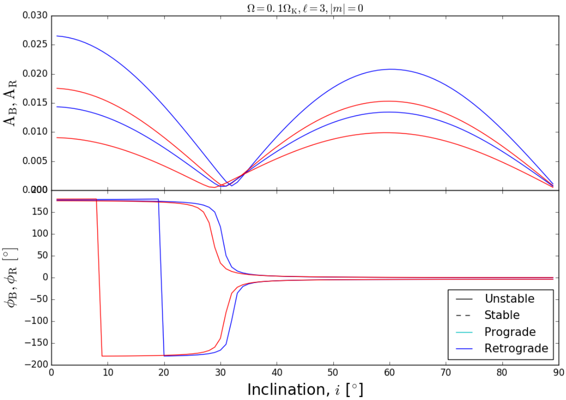

- sharp spikes result from amplitudes going to zero at different inclinations

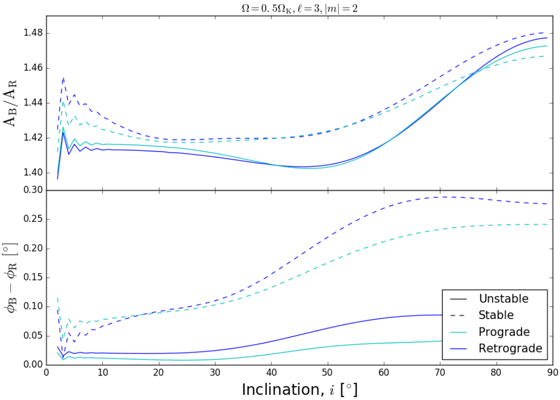

- sharp spikes result from amplitudes going to zero at different inclinations
- similar amplitude ratios and phases for modes with the same (ℓ, $|m|$) values

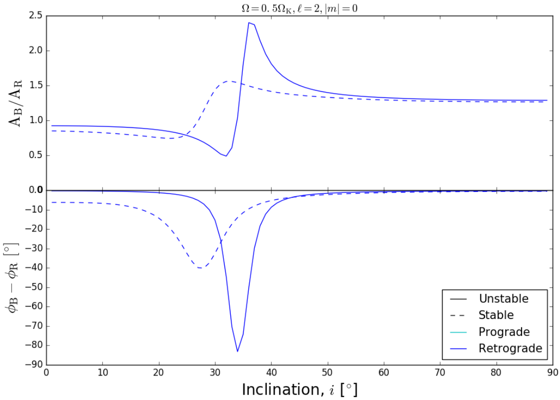

- sharp spikes result from amplitudes going to zero at different inclinations
- similar amplitude ratios and phases for modes with the same $(\ell, |m|)$ values
- but not always ...

Mode identification strategy

Mode identification strategy

- χ^2 minimisation on amplitudes and phases

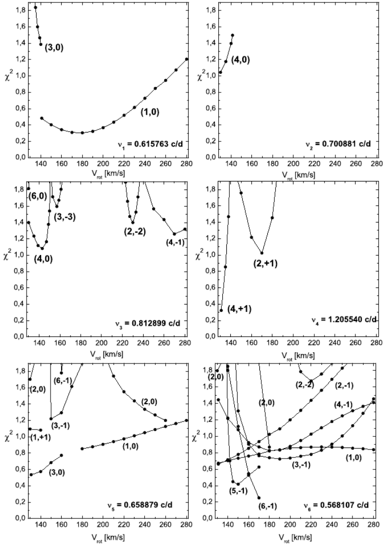

Daszyńska-Daszkiewicz et al. (2015)

α Ophiuchi

- binary system: A5III + K6V (Cowley 1969 et al. + Hinkley et al. 2011)
- $v_{eq} = 240 \mathrm{km.s}^{-1}$
- polar and equatorial radii determined through interferometry (Zhao et al. 2009)
- 57 pulsation frequencies from photometry (Monnier et al. 2010)

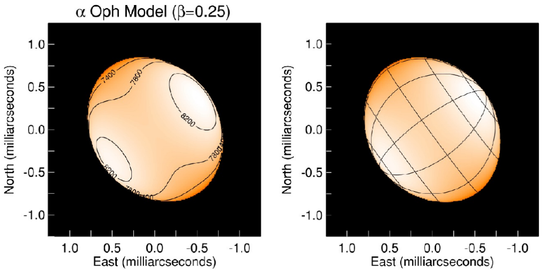

(Zhao et al. 2009)

Characteristics of the model

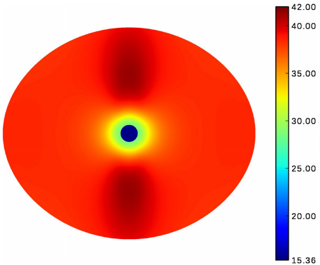

Rotation profile

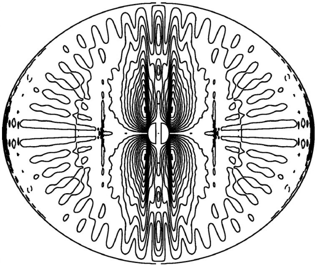

Meridional circulation

(Mirouh et al. 2013, Mirouh, PhD, 2016)

- calculated with ESTER
- mass: 2.22 $M_\odot$
- $Z = 0.02$, $X = 0.7$, $X_c = 0.26$

Mode excitation

- new fully non-adiabatic calculations

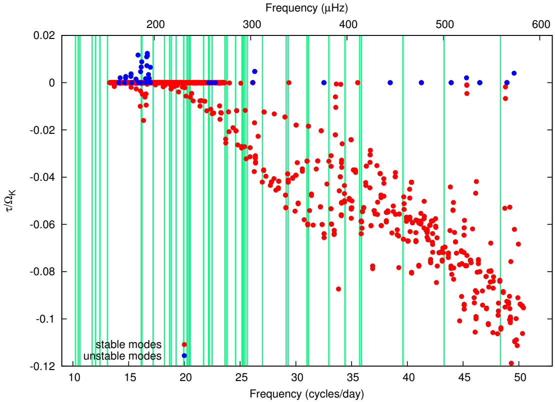

(Mirouh et al. 2017)

Mode excitation

- new fully non-adiabatic calculations
- unstable modes appear

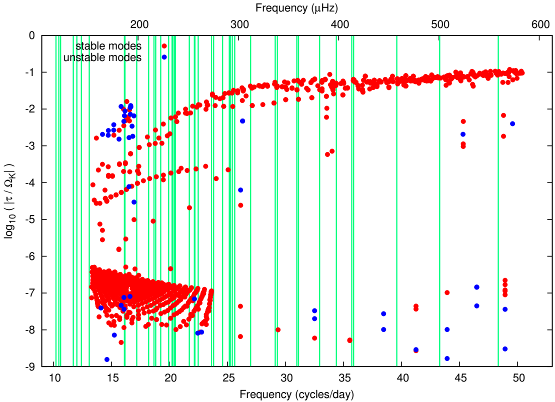

(Mirouh et al. 2017)

Mode visibilities

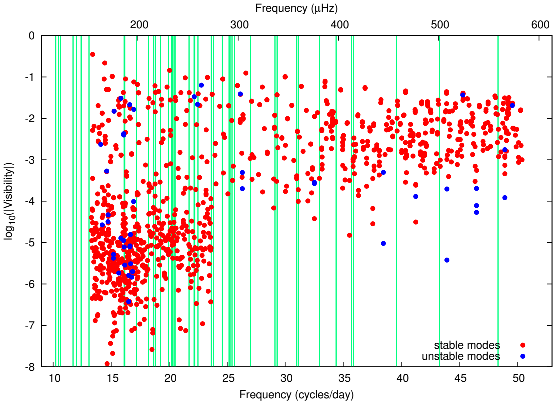

(Mirouh et al. 2017)

Conclusion

- rotation complicates mode identification techniques
- however, improved theoretical predictions
  - create database with these results
  - adapt/develop mode identification tools
- need for multicolour observations
  - BRITE, PLATO 2.0, CoRoT?, + ground follow-up

Model deformation tool

- deform 1D model by introducing centrifugal deformation
- useful for:
  - evolved models (while waiting for ESTER)
  - rapidly rotating planets
  - parametric study

- iterative process which alternates between:
  - solving Poisson's equation
  - finding level surfaces
- similar to SCF method (MacGregor et al. 2007)
- preserves $P(\rho)$ profile, but not mass

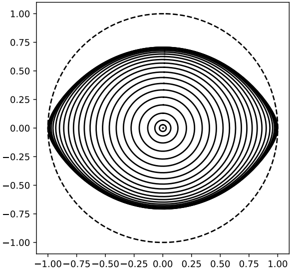

Model S at $0.9\,\Omega_K$

Model deformation tool

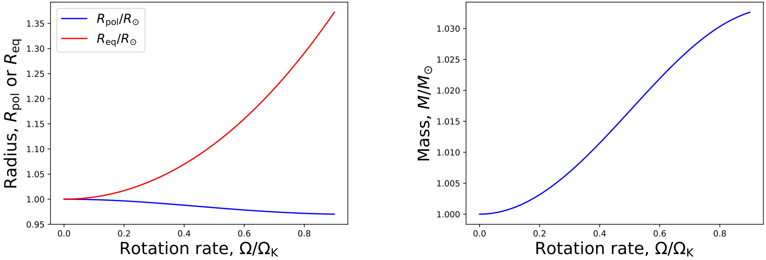

- radius and mass as a function of rotation rate

Pulsation equations

$$
\begin{aligned}
0 &= \frac{\delta\rho}{\rho_o} + \vec{\nabla}\cdot\vec{\xi} \\
0 &= \Delta\Psi - 4\pi G\left(\rho_o\frac{\delta\rho}{\rho_o} - \vec{\xi}\cdot\vec{\nabla}\rho_o\right) \\
0 &= [\omega + m\Omega]^2\,\vec{\xi} - 2i\vec{\Omega}\times[\omega+m\Omega]\,\vec{\xi} - \vec{\Omega}\times\left(\vec{\Omega}\times\vec{\xi}\right) \\
&- \vec{\xi}\cdot\vec{\nabla}\left(\varpi\Omega^2\vec{e}_\varpi\right) - \frac{P_o}{\rho_o}\vec{\nabla}\left(\frac{\delta P}{P_o}\right) + \frac{\vec{\nabla}P_o}{\rho_o}\left(\frac{\delta\rho}{\rho_o} - \frac{\delta P}{P_o}\right) - \vec{\nabla}\Psi \\
&+ \vec{\nabla}\left(\frac{\vec{\xi}\cdot\vec{\nabla}P_o}{\rho_o}\right) + \frac{\left(\vec{\xi}\cdot\vec{\nabla}P_o\right)\vec{\nabla}\rho_o - \left(\vec{\xi}\cdot\vec{\nabla}\rho_o\right)\vec{\nabla}P_o}{\rho_o^2} \\
i\,[\omega+m\Omega]\,\rho_o T_o\delta S &= \epsilon_o\rho_o\left(\cancel{\frac{\delta\epsilon}{\epsilon_o}} + \frac{\delta\rho}{\rho_o}\right) - \vec{\nabla}\cdot\delta\vec{F} \\
&+ \vec{\xi}\cdot\vec{\nabla}\left(\vec{\nabla}\cdot\vec{F}_o\right) - \vec{\nabla}\cdot\left[\left(\vec{\xi}\cdot\vec{\nabla}\right)\vec{F}_o\right] \\
\delta\vec{F}^{\mathrm{R}} &= \left[(1+\chi_T)\frac{\delta T}{T_o} + \chi_\rho\frac{\delta\rho}{\rho_o}\right]\vec{F}_o^{\mathrm{R}} \\
&- \chi_o\left[T_o\vec{\nabla}\left(\frac{\delta T}{T_o}\right) + \vec{\xi}\cdot\vec{\nabla}\left(\vec{\nabla}T_o\right) - \vec{\nabla}\left(\vec{\xi}\cdot\vec{\nabla}T_o\right)\right]
\end{aligned}
$$

- and perturbed EOS, opacities, and boundary conditions

Pulsation equations

Summary

- final result: a system of 10 equations with 10 unknowns:

$$\frac{\delta P}{P_o}, \quad \vec{\xi}, \quad \frac{\delta S}{c_\mathrm{p}}, \quad \delta \vec{F}^\mathrm{R}, \quad \frac{\delta T}{T_o}, \quad \Psi \tag{1}$$

- although some of these variables can be cancelled algebraically, they are needed to ensure good convergence

Numerical implementation

- explicit expression in spheroidal coordinates
- projection onto spherical harmonics
- radial discretisation using Chebyshev polynomials over multiple domains

N_r	N_h	Memory (in Gb)	Time (in min)	Num. proc.
400	10	3.5		
400	15	7.9		
400	20	13.4	5	4
400	29	28.0	10	8
400	40	52.7	22	8
400	50	82.3	26	16

Estimated accuracy

- the problem is stiff: reduced numerical accuracy
- estimated accuracy based on variational expression:
  - frequencies: $\sim 10^{-4}$
  - excitation/damping rates: 10^{-2} to 10^{-1}
- stability may be improved through a hybrid approach: adiabatic in the centre, non-adiabatic near the surface